Bounded Integral Controller With Limited Control Power for Nonlinear Multiple-Input Multiple-Output Systems

Yeqin Wang, *Member, IEEE*, Beibei Ren, *Senior Member, IEEE*, Qing-Chang Zhong, *Fellow, IEEE*, and Jiguo Dai, *Member, IEEE*

***Abstract*— In this brief, a bounded integral controller (BIC) with limited control power is proposed for a class of nonlinear multiple-input multiple-output (MIMO) systems. The sum-of-squares constraint on the control inputs with time-varying weights is studied and handled through the BIC design, which guarantees that both the control inputs and an auxiliary time-varying variable are dynamically constrained on a designed control circle. The BIC inherits the properties of the traditional integral controller to eliminate tracking errors and achieve disturbance rejections. Even under time-varying input weights, the BIC guarantees limited control power independently of both plant information and system states. The input-to-state (practical) stability of the closed-loop system is established. To demonstrate the effectiveness of the proposed method, experimental validations are conducted for two systems: a system with multiple dc motors subject to a power limit with time-varying input weights and a permanent magnet synchronous motor system subject to a voltage limit with time-invariant input weights.**

***Index Terms*— Bounded integral controller (BIC), limited control power, multiple-input multiple-output (MIMO), sum-of-squares constraint, time-invariant input weights, time-varying input weights.**

I. Introduction

INPUT constraints are present in many practical control systems and can be caused by physical limitations of actuators, e.g., the limited force for spacecraft rendezvous [1], the limited rotor speed for unmanned aerial vehicles (UAVs) [2] and the limited voltage for power electronics control [3], [4], or protection requirements [5]. To some extent, a bounded input design can enhance the stability of the closed-loop system [6]. For single-input single-output (SISO) systems, many approaches have been proposed to handle input constraints, e.g., the saturation unit plus antiwindup designs [7], constrained model predictive control (MPC) [8], saturated linear state feedback controller [9], constrained adaptive control [10], and optimal control design [11], [12]. A bounded integral controller (BIC) [6] is proposed to guarantee both the bounded control input and the stability of the closed-loop system. However, the problem of input constraints becomes more challenging and complicated for multiple-input multiple-output (MIMO) systems because MIMO systems have multiple channels, coupling effects, and so on. For some MIMO systems, if the input constraint is independent for each input channel, most approaches proposed for SISO systems are still applicable. However, it is more difficult to consider a constraint with multiple inputs involved, e.g., the norm constraint or the sum-of-squares constraint of all inputs [13]–[16], i.e., $\|u\| \leq \beta$ problem, where $u = [u_1, u_2, \ldots, u_n]^T \in \mathbb{R}^n$ is a general control input vector for a MIMO system with n input channels, $\|\cdot\|$ denotes the Euclidean norm, and $\beta > 0$ is a positive constant number.

In [15]–[17], $\|u\| \leq \beta$ constraint of control inputs is considered with a Takagi–Sugeno fuzzy model and solved by an optimization technique based on the linear matrix inequality (LMI) design. A similar idea based on the optimization technique subject to the LMI design is introduced into robust control of the spacecraft rendezvous to handle three-dimensional input force constraints [1]. However, the LMI method usually requires large computational efforts and is difficult to be used in real-time control systems with fast responses [3]. Moreover, the LMI-based optimization for $\|u\| \leq \beta$ constraint usually requires full model information. Apart from the LMI-based optimization, an improved integral control [4] is proposed to regulate the sum-of-squares constraint of input voltage for the vector control of induction motors.

In previous studies of MIMO systems with input constraints, e.g., the norm constraint of the control inputs discussed earlier, only the time-invariant input weights are considered. However, in some practical systems, the input constraints are subject to time-varying weights. In some cases, the maximum output capability of an actuator, e.g., a pneumatic/hydraulic cylinder, a motor, or a battery, is affected by other time-varying variables, e.g., environmental temperature. In this brief, a general sum-of-squares constraint with time-varying input weights, named "limited control power," is investigated for a class of nonlinear MIMO systems. Inspired by the BIC for SISO systems with time-invariant input constraints in [6], a new BIC is proposed in this brief to handle limited control power with time-varying input weights for nonlinear MIMO systems. A control circle is designed to make the control inputs or the final controller outputs always move and remain on the control circle to satisfy a control power limit, and the BIC is designed to realize the control circle through the Lyapunov analysis. The BIC design keeps the properties of the traditional integral controller (IC) to eliminate

Manuscript received January 13, 2020; accepted April 13, 2020. Date of publication May 6, 2020; date of current version April 12, 2021. Manuscript received in final form April 19, 2020. Recommended by Associate Editor L. Wang. *(Corresponding author: Beibei Ren.)*

Yeqin Wang was with the National Wind Institute, Texas Tech University, Lubbock, TX 79409-1021 USA. He is now with Syndem LLC, Willowbrook, IL 60527 USA (e-mail: yeqin.wang.1987@ieee.org).

Beibei Ren and Jiguo Dai are with the Department of Mechanical Engineering, Texas Tech University, Lubbock, TX 79409-1021 USA (e-mail: beibei.ren@ttu.edu; jiguo.dai@ttu.edu).

Qing-Chang Zhong is with the Department of Electrical and Computer Engineering, Illinois Institute of Technology, Chicago, IL 60616 USA (e-mail: zhongqc@ieee.org).

Color versions of one or more of the figures in this article are available online at https://ieeexplore.ieee.org.

Digital Object Identifier 10.1109/TCST.2020.2989691

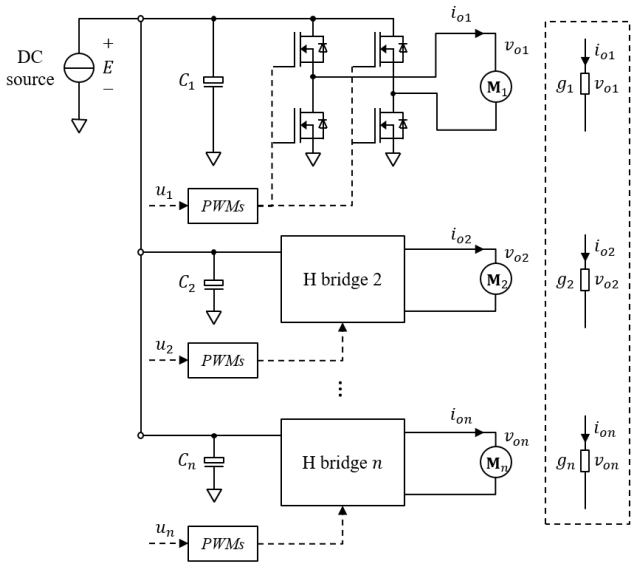

Fig. 1. System with multiple dc motors and a single source.

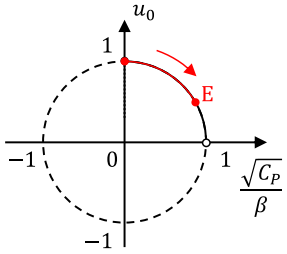

Fig. 2. Illustration of the term $(\sqrt{C_P})/\beta$ and the additional control state $u_0(t)$ moving on a control circle with the proposed BIC (6).

tracking errors and achieve disturbance rejection. Except for the information of the time-varying input weights, the BIC fulfills the desired control power limit independently from the plant information and the system states with a simple structure. The input-to-state (practical) stability (ISpS) of the closed-loop system is investigated with the small-gain theorem. It is worth mentioning that the classical saturation constraint and the standard norm constraint, $\|u\| \leq \beta$, are special cases of limited control power studied in this brief. The preliminary results of this work for the sum-of-squares constraint with time-invariant input weights are presented in [18]. In this brief, the proposed BIC with limited control power is further applied to practical systems via experimental studies, including a system with multiple dc motors with a power limit subject to time-varying input weights and a permanent magnet synchronous motor (PMSM) system with a voltage limit subject to time-invariant input weights.

The rest of this brief is organized as follows. Section II describes the problem formulation. In Section III, the BIC is developed for nonlinear MIMO systems with a control power limit. Experimental validations of both a system with multiple dc motors and a PMSM system are conducted in Section IV to demonstrate the effectiveness of the proposed BIC for limited control power with both time-varying and time-invariant input weights. Section V concludes this brief.

II. Problem Formulation With Limited Control Power

A. Practical Application Subject to a Control Power Limit

As shown in Fig. 1, a system with multiple dc motors consists of a single dc source, multiple dc motors ($\mathbf{M}_1$, $\mathbf{M}_2$, $\ldots, \mathbf{M}_n$), power converters (H-bridge 1, H-bridge 2, $\ldots$, H-bridge n), and input capacitors (C_1, C_2, $\ldots, C_n$). Each dc motor is powered by an H-bridge, which can drive the dc motor with a clockwise or counterclockwise rotation. The input capacitors are used to maintain the input dc voltage stable. This system with multiple dc motors has broad industrial applications, e.g., robotics, industrial machine tools, two/four-wheel-drive electric vehicles, and low-voltage dc systems in regular vehicles with different dc motors for windows, wipers, and fans. In these applications, the single dc source can be a battery or a power electronic device fed by other power sources, e.g., the utility grid. It is known that both batteries and power electronic devices have limited power outputs. If the power output limit is violated, the lifespan of the source can be reduced, or damages are caused. Though some protections with detection and shutdown can be adopted to handle this problem in traditional designs, the protection performance is restricted by the response time and the designed tolerance.

For this system with multiple dc motors, the control objectives can be motor speeds, motor torques, or motor positions depending on the application. The control inputs are the duty cycles u_i of the H-bridge converters, with $u_i \in [-1, 1]$. The power limitation of the dc source can be regarded as the total limited output power of the H-bridge converters, which is expressed as

$$P_{\text{total}} = \sum_{i=1}^{n} i_{oi}(t) v_{oi}(t) \leq P_{\max} \tag{1}$$

where P_{total} is the total output power of the H-bridge converters, $P_{\max}$ is the power limit of the source, and i_{oi} and v_{oi} are the output current and the output voltage of the H-bridge converters, respectively. According to the characteristics of the H-bridge converters, the output voltages of the H-bridge converters can be approximately expressed as $v_{oi}(t) = u_i(t)E(t)$, where $E(t)$ is the voltage of the dc source. Then, the power constraint (1) can be rewritten as

$$\sum_{i=1}^{n} g_i(t) E^2(t) u_i^2(t) \leq P_{\max} \tag{2}$$

where $g_i(t) = (i_{oi}(t))/(v_{oi}(t))$ are the equivalent time-varying conductance of the dc motors. In this power constraint (2), $g_i(t)E^2(t) > 0$ are regarded as time-varying input weights, which can be directly or indirectly measured.

B. Problem Formulation

Following the above mentioned practical application, in this brief, a control problem subject to limited control power is formulated and investigated for a class of nonlinear MIMO

systems described as

$$\begin{aligned}\dot{x}_1 &= f_1(x_1, x_2, \ldots, x_n, u_1) + d_1\\ \dot{x}_2 &= f_2(x_1, x_2, \ldots, x_n, u_2) + d_2\\ &\vdots\\ \dot{x}_n &= f_n(x_1, x_2, \ldots, x_n, u_n) + d_n\end{aligned} \tag{3}$$

where $x_i = [x_{i1}, x_{i2}, \ldots, x_{im_i}]^T \in \mathbb{R}^{m_i}$, $i = 1, 2, \ldots, n$, are system state vectors. The dimensions m_i of x_i are determined by each subsystem, and f_i are system dynamics that are assumed to be ISpS, which is practical because many engineering systems have an inherent dissipative structure [6]. $d_i(t) \in \mathbb{R}^{m_i}$ are bounded external disturbance vectors with the same dimensions as x_i, and $u_i(t) \in \mathbb{R}$ are the control inputs. The system output y is defined as $y = [x_{11}, x_{21}, \ldots, x_{n1}]^T$. Without loss of generality, the control input $u = [u_1, u_2, \ldots, u_n]^T$ is subject to limited control power

$$C_P = \sum_{i=1}^{n} c_i(t)u_i^2(t) \le \beta^2 \tag{4}$$

where C_P is the control power of the system, $c_i(t) > 0$ are known or measurable differentiable time-varying weights for $u_i(t)$, and $\beta > 0$ is a positive constant. For simplicity, the index i, which varies from 1 to n, for the summation notation $\sum$ is omitted in the rest of this brief.

The control objective is to design a controller for the MIMO system (3) such that the system output $y = [x_{11}, x_{21}, \ldots, x_{n1}]^T$ can asymptotically track its reference $r = [x_{11}^{\text{ref}}, x_{21}^{\text{ref}}, \ldots, x_{n1}^{\text{ref}}]^T$ subject to limited control power (4). In other words, the tracking errors $e_i(t) = x_{i1}^{\text{ref}} - x_{i1}$, $i = 1, 2, \ldots, n$, can converge to zero as $t \to \infty$.

Note that, in addition to the power limit, the constraint (4) also can represent other actuator physical limitations, e.g., force limitation, voltage limitation, and so on.

III. BIC Design for MIMO Systems With Limited Control Power

In the preliminary version of this brief [18], the sum-of-squares constraint with time-invariant input weights is studied for MIMO systems. In this brief, the results in [18] are further extended to nonlinear MIMO systems subject to limited control power with time-varying input weights, i.e., $\sum c_i(t)u_i^2(t) \le \beta^2$. The ISpS stability of the closed-loop system, performance analysis, and discrete implementation are investigated.

A. Controller Design

The requirements of limited control power (4) can be achieved if the control inputs or the final controller outputs u_i can always move and remain on a control circle shown in Fig. 2, which can be described as

$$\left(\frac{\sqrt{C_P}}{\beta}\right)^2 + u_0^2(t) = 1 \tag{5}$$

where $u_0(t)$ is an additional auxiliary time-varying control variable.

In order to achieve the desired control circle (5) and asymptotic reference tracking with $e_i(t) \to 0$, a dynamic controller is developed for the final controller outputs u_i and the auxiliary time-varying variable u_0 as

$$\begin{aligned}\dot{u}_1(t) &= -k\left[\frac{\sum c_i(t)u_i^2(t)}{\beta^2} + u_0^2(t) - 1\right]u_1(t) + k_1u_0^2(t)e_1\\ \dot{u}_2(t) &= -k\left[\frac{\sum c_i(t)u_i^2(t)}{\beta^2} + u_0^2(t) - 1\right]u_2(t) + k_2u_0^2(t)e_2\\ &\vdots\\ \dot{u}_n(t) &= -k\left[\frac{\sum c_i(t)u_i^2(t)}{\beta^2} + u_0^2(t) - 1\right]u_n(t) + k_nu_0^2(t)e_n\\ \dot{u}_0(t) &= -k\left[\frac{\sum c_i(t)u_i^2(t)}{\beta^2} + u_0^2(t) - 1\right]u_0(t)\\ &\quad - \frac{c_1(t)u_1(t)}{\beta^2}k_1u_0(t)e_1 - \frac{c_2(t)u_2(t)}{\beta^2}k_2u_0(t)e_2\\ &\quad - \cdots - \frac{c_n(t)u_n(t)}{\beta^2}k_nu_0(t)e_n\\ &\quad - \frac{\dot{c}_1(t)u_1^2(t)}{2u_0(t)\beta^2} - \frac{\dot{c}_2(t)u_2^2(t)}{2u_0(t)\beta^2} - \cdots - \frac{\dot{c}_n(t)u_n^2(t)}{2u_0(t)\beta^2}\end{aligned} \tag{6}$$

where k is a positive constant, e_i ($i = 1, \ldots, n$) are the system output tracking errors, and k_i are integral gains. It can be noted that the proposed controller is an improved version of the traditional IC. It inherits the properties of the IC with the dynamic integral gain $k_iu_0^2(t)$ to eliminate tracking errors.

Lemma 1: The BIC design in (6) achieves both the control circle (5) and the requirement of limited control power (4).

Proof: Consider the following Lyapunov function candidate:

$$V(t) = \frac{\sum c_i(t)u_i^2(t)}{\beta^2} + u_0^2(t). \tag{7}$$

Taking the time derivative of $V(t)$ along with (6), it yields

$$\begin{aligned}\dot{V}(t) &= \frac{\sum \dot{c}_i(t)u_i^2(t)}{\beta^2} + \frac{\sum 2c_i(t)u_i(t)\dot{u}_i(t)}{\beta^2} + 2u_0(t)\dot{u}_0(t)\\ &= \frac{\dot{c}_1(t)u_1^2(t)}{\beta^2} + \frac{\dot{c}_2(t)u_2^2(t)}{\beta^2} + \cdots \frac{\dot{c}_n(t)u_n^2(t)}{\beta^2}\\ &\quad - \frac{2kc_1(t)u_1^2(t)}{\beta^2}[V(t) - 1] + \frac{2c_1(t)u_1(t)}{\beta^2}k_1e_1u_0^2(t)\\ &\quad - \frac{2kc_2(t)u_2^2(t)}{\beta^2}[V(t) - 1] + \frac{2c_2(t)u_2(t)}{\beta^2}k_2e_2u_0^2(t)\\ &\quad \vdots\\ &\quad - \frac{2kc_n(t)u_n^2}{\beta^2}[V(t) - 1] + \frac{2c_n(t)u_n(t)}{\beta^2}k_ne_nu_0^2(t)\\ &\quad - 2ku_0^2(t)[V(t) - 1] - \frac{2c_1(t)u_1(t)}{\beta^2}k_1e_1u_0^2(t)\\ &\quad - \frac{2c_2(t)u_2(t)}{\beta^2}k_2e_2u_0^2(t)\\ &\quad - \cdots - \frac{2c_n(t)u_n(t)}{\beta^2}k_ne_nu_0^2(t)\\ &\quad - 2u_0(t)\left[\frac{\dot{c}_1(t)u_1^2(t)}{2u_0(t)\beta^2} + \frac{\dot{c}_2(t)u_2^2(t)}{2u_0(t)\beta^2} + \cdots + \frac{\dot{c}_n(t)u_n^2(t)}{2u_0(t)\beta^2}\right]\\ &= -2kV(t)[V(t) - 1]\\ &= -2kV^2(t) + 2kV(t).\end{aligned} \tag{8}$$

Solving (8) gives

$$V(t) = \frac{e^{2kt}V(0)}{e^{2kt}V(0) - V(0) + 1} = \frac{1}{1 - e^{-2kt}\left(1 - \frac{1}{V(0)}\right)}. \quad (9)$$

With the proper initial designs, e.g., with $u_0(0) = 1$ and $u_i(0) = 0$, there is $V(0) = 1$. As a result

$$V(t) = 1 \quad \forall \quad t \geq 0.$$

Consequently, it always holds true that $(\sum c_i(t)u_i^2(t))/(\beta^2) + u_0^2(t) = 1$ for the control circle shown in Fig. 2. Hence, the limited control power (4) is fulfilled. This completes the proof. ■

It is interesting to note that $V(t)$ still can converge to 1 as $t \to \infty$ if $V(0)$ is not equal to zero, according to (9). The rate of convergence can be adjusted by the parameter k. Therefore, the terms $-k[(\sum c_i(t)u_i^2(t))/(\beta^2) + u_0^2(t) - 1]u_i(t)$ introduced in the proposed BIC (6) are used to handle measurement noises, parameter drifts, and numerical errors in practical implementations, where (5) can always hold to guarantee limited control power (4). If $V(t)$ converges to 1, the term $\sqrt{C_P}/\beta$ and the additional state $u_0(t)$ always remain on the first quadrant of the control circle. At the steady state, $\dot{u}_i(t)$ and $\dot{u}_0(t)$ are regulated to 0, and the BIC operates at the equilibrium point, e.g., point E indicated in Fig. 2.

Even under the time-varying input weights $c_i(t)$, the limited control power (4) is guaranteed through the proposed BIC (6), and the effects from system states are also relaxed.

B. Closed-Loop System Stability

Considering the plant (3) and the BIC (6), the closed-loop system can be represented as an interconnected form with two subsystems, Σ_1 and Σ_2, as shown in Fig. 3, where $y = [x_{11}, x_{21}, \ldots, x_{n1}]^T$ and $u = [u_1, u_2, \ldots, u_n]^T$ are internal vectors and $d = [d_1^T, d_2^T, \ldots, d_n^T]^T$ and $r(t) = [x_{11}^{\text{ref}}, x_{21}^{\text{ref}}, \ldots, x_{n1}^{\text{ref}}]^T$ are external input vectors.

Theorem 1: The closed-loop system shown in Fig. 3 as designed earlier is ISpS with respect to both inputs $d(t)$ and $r(t)$ if the plant (3) is ISpS with respect to inputs $d(t)$ and $u(t)$.

Proof: For the subsystem Σ_1 with ISpS, there exists a class $\mathcal{KL}$ function $\beta_{kl1}(\cdot)$, class $\mathcal{K}_\infty$ functions $\gamma_u(\cdot)$ and $\gamma_d(\cdot)$, and positive constants K_1, K_2, and K_3 such that for any state $y(0)$ with $\|y(0)\| < K_1$, any input $u(t)$ with $\sup_{t\geq 0}\|u(t)\| < K_2$, and any external input $d(t)$ with $\sup_{t\geq 0}\|d(t)\| < K_3$, there is

$$\|y(t)\| \leq \beta_{kl1}(\|y(0)\|, t) + \gamma_u\Big(\sup_{0\leq \tau \leq t}\|u(\tau)\|\Big) + \gamma_d\Big(\sup_{0\leq \tau \leq t}\|d(\tau)\|\Big) + \alpha_1$$

for all $t \geq 0$, where $\alpha_1 \geq 0$ is a constant.

Through the BIC design in (6), the output of Σ_2 satisfies

$$\sum c_i(t)u_i^2(t) \leq \beta^2.$$

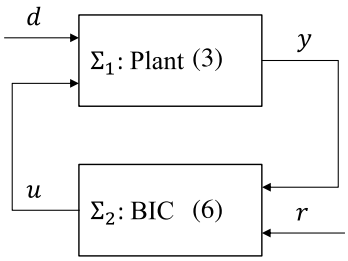

Fig. 3. Interconnection form of the closed-loop system.

Consequently, there is

$$\|u(t)\| \leq \frac{\beta}{\sqrt{c_{\min}}}$$

where $c_{\min} = \min_t\{c_i(t)\} > 0$.

For the subsystem Σ_2, there exists a class $\mathcal{KL}$ function $\beta_{kl2}(\cdot)$, class $\mathcal{K}_\infty$ functions $\gamma_y(\cdot)$ and $\gamma_r(\cdot)$, and positive constants K_4, K_5, and K_6 such that for any state $u(0)$ with $\|u(0)\| < K_4$, any input $y(t)$ with $\sup_{t\geq 0}\|y(t)\| < K_5$, and any external input $r(t)$ with $\sup_{t\geq 0}\|r(t)\| < K_6$, there is

$$\begin{aligned}\|u(t)\| &\leq \frac{\beta}{\sqrt{c_{\min}}} \\ &\leq \beta_{kl2}(\|u(0)\|, t) + \gamma_y\Big(\sup_{0\leq \tau \leq t}\|y(\tau)\|\Big) \\ &\quad + \gamma_r\Big(\sup_{0\leq \tau \leq t}\|r(\tau)\|\Big) + \alpha_2 \end{aligned} \quad (10)$$

for all $t \geq 0$, where $\alpha_2 = \beta/\sqrt{c_{\min}}$ is a positive constant.

Then, two $\mathcal{K}_\infty$ functions ρ_1 and ρ_2 and a nonnegative real number s_l can be found to achieve

$$\left.\begin{aligned}(I_d + \rho_2) \circ \gamma_y \circ (I_d + \rho_1) \circ \gamma_u(s) \leq s \\ (I_d + \rho_1) \circ \gamma_u \circ (I_d + \rho_2) \circ \gamma_y(s) \leq s\end{aligned}\right\} \forall s \geq s_l$$

where I_d is the identity function, and $\circ$ is the function composition, as γ_y can be designed small enough, according to (10). By applying the small-gain theorem in [19], the closed-loop system is ISpS with respect to the external inputs $d(t)$ and $r(t)$. This completes the proof. ■

C. Performance Analysis

When $V(t)$ in (7) is equal to 1, the BIC (6) is reduced to

$$\begin{aligned}\dot{u}_i(t) &= k_i u_0^2(t) e_i \qquad (i = 1, \ldots, n) \\ \dot{u}_0(t) &= -\frac{c_1(t)u_1(t)}{\beta^2}k_1 e_1 u_0(t) - \frac{c_2(t)u_2(t)}{\beta^2}k_2 e_2 u_0(t) \\ &\quad - \cdots - \frac{c_n(t)u_n(t)}{\beta^2}k_n e_n u_0(t) \\ &\quad - \frac{\dot{c}_1(t)u_1^2(t)}{2u_0(t)\beta^2} - \frac{\dot{c}_2(t)u_2^2(t)}{2u_0(t)\beta^2} - \cdots - \frac{\dot{c}_n(t)u_n^2(t)}{2u_0(t)\beta^2}.\end{aligned}$$

Each subcontroller is an IC with a dynamic integral gain $k_i u_0^2(t)$. As long as $u_0(t)$ does not converge to 0, the ICs can handle step disturbances and step references and eliminate tracking errors, according to the internal model principle, since the subsystems f_i are ISpS.

D. Special Cases

In this brief, the BIC (6) is proposed for MIMO systems under a single constraint of all control inputs with time-varying weights $c_i(t)$. The results are also applicable to the special case when the weights $c_i(t)$ are time-invariant. This can be easily verified when $\dot{c}_i$ are set as zero in both the control law (6) and the Lyapunov analysis (8). The preliminary results of this special case are presented in [18]. Especially, when $c_i = 1$, the problem is reduced to a standard norm constraint problem with $\|u\| \le \beta$.

It is also applicable to MIMO systems with multiple input constraints. For example, when the control inputs $u_i(t)$ are divided into N groups with each group having M_j control inputs, $j = 1, 2, \ldots, N$, subject to limited control power defined as

$$\begin{aligned} C_{P1} &= \sum_{k1=1}^{M_1} c_{k1}(t)u_{k1}^2(t) \le \beta_1^2 \\ C_{P2} &= \sum_{k2=1}^{M_2} c_{k2}(t)u_{k2}^2(t) \le \beta_2^2 \\ &\vdots \\ C_{PN} &= \sum_{kN=1}^{M_N} c_{kN}(t)u_{kN}^2(t) \le \beta_N^2 \end{aligned}$$

where $c_{kj}(t) > 0$ are known differentiable time-varying weights for control inputs $u_{kj}(t)$ and $\beta_j > 0$, which are positive constants, the proposed BIC (6) can be adopted N times to handle these N groups of constraints. If $M_j = 1$, $c_{kj} = 1$, the multiple constraints are reduced to a classical saturation constraint problem, i.e., $|u_i| \le \beta_i$.

E. Discrete Implementation

Instead of the differential form of the proposed BIC in (6), the integral form is used for the discrete implementation of (6) for practical applications. For example, (6) can be implemented as

$$\begin{aligned} u_i(m+1) &= u_i(m) + T\big[-k\eta(m)u_i(m) + k_i u_0^2(m)e_i(m)\big] \\ u_0(m+1) &= u_0(m) + T\Bigg[-k\eta(m)u_0(m) \\ &\quad - \sum \frac{c_i(m)u_i(m)}{\beta^2} k_i u_0(m)e_i(m) \\ &\quad - \sum \frac{\delta_i(m)u_i^2(m)}{2u_0(m)\beta^2}\Bigg] \end{aligned}$$

through the forward Euler method, where $\eta(m) = (\sum c_i(m)u_i^2(m))/(\beta^2) + u_0^2(m) - 1$, $\delta_i(m)$ is the derivative of $c_i(m)$, $i = 1, 2, \ldots, n$, m is the sample index, and T is the sampling period of the digital controller.

In practical applications, in order to eliminate the measurement noise, $\dot{c}_i(t)$ can be numerically approximated via low-pass filters [20] as

$$\tilde{c}_i(t) = L^{-1}\left\{\frac{\Omega_i}{s+\Omega_i}\right\} * c_i(t)$$

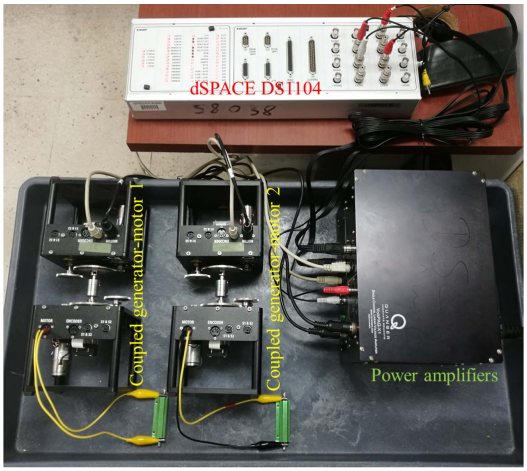

Fig. 4. Experimental test rig for a system with multiple dc motors.

where L^{-1} means the inverse Laplace transformation, and $*$ is the convolution operator. Then

$$\dot{c}_i(t) \approx \dot{\tilde{c}}_i(t) = \Omega_i[c_i(t) - \tilde{c}_i(t)].$$

They can be digitally implemented as

$$\begin{aligned} \tilde{c}_i(m+1) &= (1 - T\Omega_i)\tilde{c}_i(m) + T\Omega_i c_i(m) \\ \delta_i(m) &= \Omega_i[c_i(m) - \tilde{c}_i(m)]. \end{aligned}$$

It is worth noting that, as long as the sampling frequency is high enough for the digital controller, the discrete implementation can achieve similar performance as in the continuous time domain. The terms $-k[(\sum c_i(t)u_i^2(t))/(\beta^2) + u_0^2(t) - 1]u_i(t)$ in (6) can help eliminate numerical errors in the discrete implementation, as discussed in Section III-A.

IV. Experimental Validation

A. Case I: Limited Control Power With Time-Varying Input Weights

To validate the proposed BIC for MIMO systems subject to limited control power with time-varying input weights, a system with multiple dc motors, discussed in Section II-A, is investigated. An experimental test rig with two motor–generator sets is built up, as shown in Fig. 4. There are two motors driving two generators individually. Both motors are controlled by a single controller, a dSPACE DS1104 kit. Instead of the H-bridge converters discussed in Section II-A, power amplifiers are used to drive the dc motors. The control signals are sent from the dSPACE DS1104 to the power amplifiers. The generator connected to a 1 Ω resistor is performed as the load for the dc motor in each motor–generator set. The mathematical model of this system is given as [21]

$$J_{mi}\dot{\omega}_i = T_{ei} - T_{li} \ (i = 1, 2) \tag{11}$$

$$L_{mi}\dot{i}_{oi} = -R_{mi}i_{oi} - k_{\omega i}\omega_i + v_{oi} \tag{12}$$

where ω_i is the motor speed, i_{oi} is the armature current, J_{mi} is the equivalent total moment of inertia of the rotor, $T_{ei} = k_{ti}i_{oi}$ is the electromagnetic torque of the dc motor, T_{li} is the total load including the rolling friction and the load from

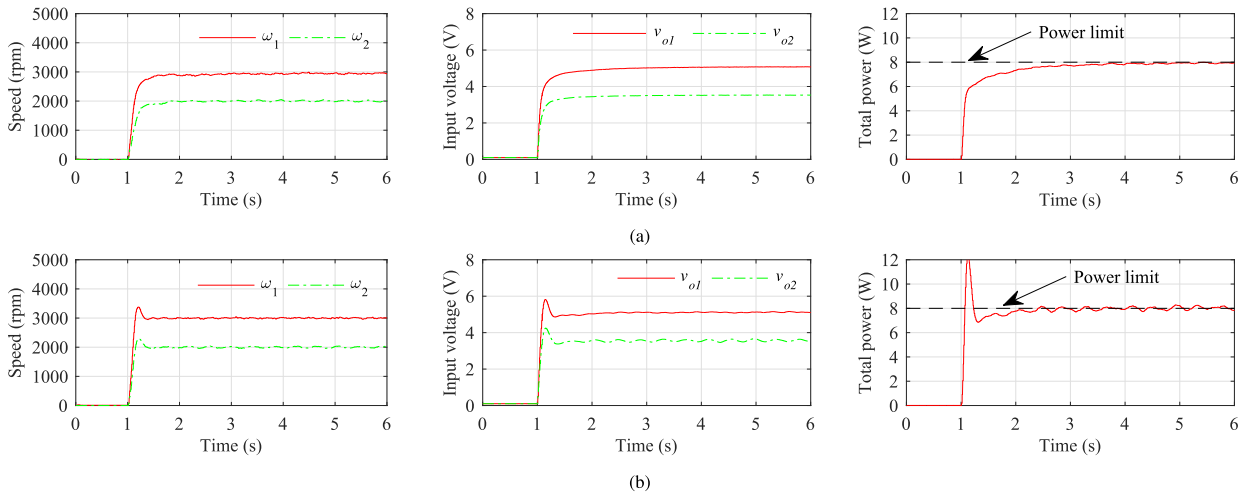

Fig. 5. Experimental results for the control of multiple dc motors with motor speed (left column), motor input voltage (middle column), and total power P_{total} (right column). (a) With the proposed BIC. (b) With the traditional IC.

TABLE I
CONTROL PARAMETERS FOR CASE I

Parameters	Values	Parameters	Values
$k_{\omega 1}$, $k_{\omega 2}$	1/40	P_{max}	8 W
k	1000	Ω_1, Ω_2	1000

the generator side, L_{mi} is the armature inductance, R_{mi} is the armature resistance, $k_{ti} = k_{\omega i}$ is the torque constant or voltage constant, and v_{oi} is the voltage input. More information of system modeling can be found in [21].

The speed control of the two dc motors is considered in this experiment. Similar to the power limitation for the total output power of the H-bridge converters in Section II-A, the total output power of the amplifiers is subject to a limit

$$P_{\text{total}} = \sum_{i=1}^{2} i_{oi}(t) v_{oi}(t) \le P_{\max}.$$

Again, it can be further rewritten as

$$\sum_{i=1}^{2} g_i(t) v_{oi}^2(t) \le P_{\max} \tag{13}$$

where $g_i(t) = (i_{oi}(t))/(v_{oi}(t))$ can be measured by the dSPACE DS1104 kit. In order to achieve both speed regulation and satisfy the condition (13), the proposed BIC (6) is implemented on the dSPACE DS1104 kit with the sampling frequency of 10 kHz. The control parameters are shown in Table I.

The speed references of the two dc motors are 3000 rpm and 2000 rpm, respectively. The system responses are shown in Fig. 5 with the BIC in Fig. 5(a) and the traditional IC in Fig. 5(b). For clarity, unlike the duty cycles for the H-bridge converters discussed in Section II-A, the control inputs v_{o1} and v_{o2} are input voltages of the dc motors. Both BIC and traditional IC can achieve similar desired control performances at the steady state. Compared with the traditional IC in Fig. 5(b), the BIC shown in Fig. 5(a) does not have

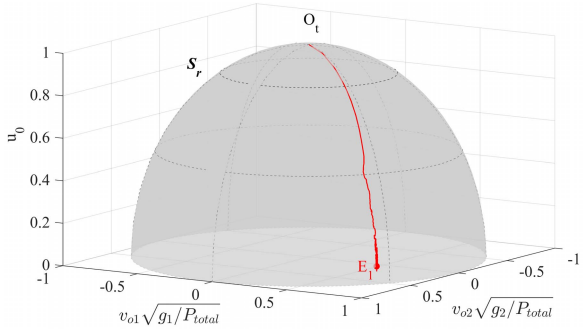

Fig. 6. Moving controller states with the proposed BIC for the control of two DC motors.

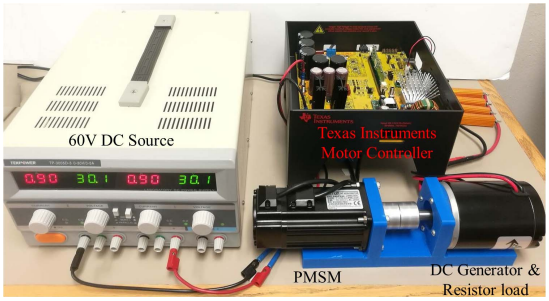

Fig. 7. Experimental test rig for a PMSM system.

any overshoots in both motor speeds and control inputs. The BIC can always regulate the total power P_{total} within the limit, whereas the traditional IC violates the power limit at both the transient state and the steady state. The operations of the control inputs and the additional state u_0 are illustrated in Fig. 6, where the controller states remain on a controller sphere S_r by using the proposed BIC (6) and converge to a small neighborhood of point E_1 at the steady state. In summary, the BIC demonstrates good reference tracking performances and capabilities to handle limited control power with time-varying input weights.

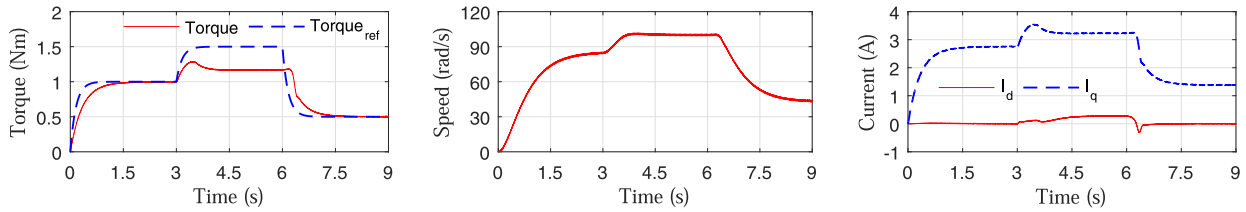

Fig. 8. Experimental results of the vector control for a PMSM with the proposed BIC. (a) Motor torque. (b) Motor mechanical speed. (c) Motor dq currents.

B. Case II: Limited Control Power With Time-Invariant Input Weights

To further validate the proposed BIC for MIMO systems subject to limited control power with time-invariant input weights, the vector control of a PMSM with a voltage limit is investigated through experimental studies. The experimental test rig is shown in Fig. 7, where an Anaheim Automation EMJ-04 PMSM is driven by a Texas Instruments (TI) motor controller. A dc source is used to supply dc power for the TI motor controller. An AmpFlow E30-150 dc generator plus four parallel-connected resistors (total 0.25 Ω) are performed as the mechanical loads for the PMSM. The electrical model of a PMSM in the dq reference frame is given as [22]

$$\dot{i}_d = -\frac{R_s}{L_d} i_d + \frac{\omega_e L_q}{L_d} i_q + \frac{1}{L_d} U_d$$
$$\dot{i}_q = -\frac{R_s}{L_q} i_q - \frac{\omega_e L_d}{L_q} i_d + \frac{1}{L_q} U_q - \frac{\omega_e \psi_f}{L_q}$$

where i_d and i_q are stator currents, U_d and U_q are the stator voltage inputs, L_d and L_q are stator winding inductance, R_s is the stator winding resistance, ψ_f is the core magnetic flux, and ω_e is the electrical angular velocity. The voltage inputs U_d and U_q are limited by both the dc-bus voltage $\mathrm{V_{dc}}$ and the adopted pulse width modulation (PWM) method. Usually, the limited voltage for the voltage inputs U_d and U_q can be expressed as

$$\sqrt{u_d^2 + u_q^2} \leq 1 \tag{14}$$

where u_d and u_q are the normalized values of U_d and U_q, respectively. Note that this constraint is the special case of limited control power (4), and $c_i(t)$ are constants, as discussed in Section III-D.

The mechanical model of the PMSM is

$$J_m \dot{\omega} = T_e - T_l$$

where $\omega = (\omega_e / p)$ is the mechanical rotational speed, p is the number of pole pairs, J_m is the rotational moment of inertia, T_e is the electromagnetic torque of the PMSM, and T_l is the total load including the rolling friction and the load from the generator side. In this brief, a surface-mounted magnet type PMSM is considered with $L_d = L_q$. Therefore, the electromagnetic torque is calculated as

$$T_e = \frac{3}{2} p \psi_f i_q. \tag{15}$$

The nominal system parameters are shown in Table II. In this brief, the torque control of the PMSM is considered as the torque regulation is usually adopted to control PMSM in many applications, e.g., electric vehicles and wind turbines.

TABLE II
SYSTEM PARAMETERS FOR CASE II

Parameters	Values	Parameters	Values
ψ_f	0.06 V·s/rad	$\mathrm{V_{dc}}$	60 V
p	4	PWM frequency	20 kHz

In practice, the current is often controlled to generate a desired torque for a PMSM, e.g., the i_q reference can be set as $2T_e/(3p\psi_f)$ to achieve the desired electromagnetic torque, according to (15), and the i_d reference can be set as 0. The proposed BIC (6) is conducted on a TI TMS320F28335 microcontroller for PMSM control, where the sampling frequency is set as 10 kHz. Note that $\dot{c}_i(t) = 0$ is adopted in the implementation of the proposed BIC (6) in this special case. Other control parameters are selected as $k_d = 1000$, $k_q = 1000$, and $k = 1000$.

The system responses are illustrated in Figs. 8 and 9. Initially, the electromagnetic torque reference is set to 1 N · m by passing through a first-order low-pass filter. The electromagnetic torque of the PMSM can track its reference well, as shown in Fig. 8(a), where the mean absolute error (MAE) of the electromagnetic torque tracking during 2.9 $\sim$ 3 s is about 0.0019 N · m. The motor speed converges to its steady state within about 1.5 s, as shown in Fig. 8(b). The motor currents are shown in Fig. 8(c), wherein i_d is well regulated to 0, and i_q is regulated to a positive number to generate the positive torque. The motor voltages are shown in Fig. 9(a) with the negative u_d and the positive u_q. At $t = 3$ s, the torque reference is changed to 1.5 N · m, and $(u_d^2 + u_q^2)^{1/2}$ increases to the maximum value quickly. Though the electromagnetic torque cannot be regulated because of the voltage limit, the BIC still regulates $(u_d^2 + u_q^2)^{1/2}$ within the limit, as shown in Fig. 9(a), and the closed-loop system still keeps stable operation. When the torque reference is set to 0.5 N · m at $t = 6$ s, both electromagnetic torque and motor currents are well regulated again, due to the decrease in $(u_d^2 + u_q^2)^{1/2}$, where the MAE of the electromagnetic torque tracking during 8.8 $\sim$ 9 s is about 0.0036 N · m. The motor speed decreases with a lower torque. The BIC can always keep $(u_d^2 + u_q^2)^{1/2} \leq 1$ at different stages and guarantee system stability. The controller states u_d, u_q, and u_0 are illustrated in Fig. 9(b), where the controller states remain on a controller sphere S_r with the proposed BIC (6). The small neighborhoods of the equilibrium points E_1, E_2, and E_3 represent three steady states of the system, during 2 $\sim$ 3 s,

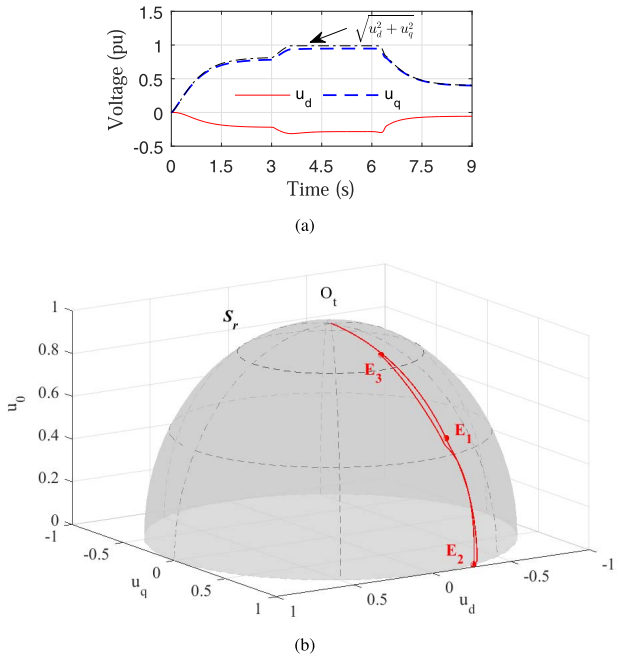

Fig. 9. Motor dq voltage inputs with the proposed BIC for the vector control of a PMSM. (a) In the time domain. (b) Moving on a controller sphere.

5 ∼ 6 s, and 8 ∼ 9 s, respectively. Therefore, the BIC can achieve good reference tracking and handle limited control power with time-invariant input weights in this experimental study.

V. Conclusion

A BIC with limited control power has been proposed for a class of nonlinear MIMO systems in this brief. The control power limit on the control inputs with both time-varying and time-invariant weights has been achieved through the bounded controller design. The ISpS of the closed-loop system has been proven based on the small-gain theorem. Experimental validations on a system with multiple dc motors subject to a power limit with time-varying input weights and a PMSM system subject to a voltage limit with time-invariant input weights have been provided to validate the proposed BIC.

References

[1] H. Gao, X. Yang, and P. Shi, "Multi-objective robust H_∞ control of spacecraft rendezvous," *IEEE Trans. Control Syst. Technol.*, vol. 17, no. 4, pp. 794–802, Jul. 2009.

[2] N. Cao and A. F. Lynch, "Inner–outer loop control for quadrotor UAVs with input and state constraints," *IEEE Trans. Control Syst. Technol.*, vol. 24, no. 5, pp. 1797–1804, Sep. 2016.

[3] T. Tarczewski and L. M. Grzesiak, "Constrained state feedback speed control of PMSM based on model predictive approach," *IEEE Trans. Ind. Electron.*, vol. 63, no. 6, pp. 3867–3875, Jun. 2016.

[4] G. C. Konstantopoulos, A. T. Alexandridis, and E. D. Mitronikas, "Bounded nonlinear stabilizing speed regulators for VSI-fed induction motors in field-oriented operation," *IEEE Trans. Control Syst. Technol.*, vol. 22, no. 3, pp. 1112–1121, May 2014.

[5] T. Meng and W. He, "Iterative learning control of a robotic arm experiment platform with input constraint," *IEEE Trans. Ind. Electron.*, vol. 65, no. 1, pp. 664–672, Jan. 2018.

[6] G. C. Konstantopoulos, Q.-C. Zhong, B. Ren, and M. Krstic, "Bounded integral control of input-to-state practically stable nonlinear systems to guarantee closed-loop stability," *IEEE Trans. Autom. Control*, vol. 61, no. 12, pp. 4196–4202, Dec. 2016.

[7] S. Tarbouriech and M. Turner, "Anti-windup design: An overview of some recent advances and open problems," *IET Control Theory Appl.*, vol. 3, no. 1, pp. 1–19, Jan. 2009.

[8] M. Böck and A. Kugi, "Constrained model predictive manifold stabilization based on transverse normal forms," *Automatica*, vol. 74, pp. 315–326, Dec. 2016.

[9] B. Zhou and J. Lam, "Global stabilization of linearized spacecraft rendezvous system by saturated linear feedback," *IEEE Trans. Control Syst. Technol.*, vol. 25, no. 6, pp. 2185–2193, Nov. 2017.

[10] N. E. Kahveci and P. A. Ioannou, "Adaptive steering control for uncertain ship dynamics and stability analysis," *Automatica*, vol. 49, no. 3, pp. 685–697, Mar. 2013.

[11] K. Graichen, A. Kugi, N. Petit, and F. Chaplais, "Handling constraints in optimal control with saturation functions and system extension," *Syst. Control Lett.*, vol. 59, no. 11, pp. 671–679, Nov. 2010.

[12] D. W. Kim, "Tracking of REMUS autonomous underwater vehicles with actuator saturations," *Automatica*, vol. 58, pp. 15–21, Aug. 2015.

[13] M. Corless and G. Leitmann, "Bounded controllers for robust exponential convergence," *J. Optim. Theory Appl.*, vol. 76, no. 1, pp. 1–12, Jan. 1993.

[14] W. Jiang, H. Wang, J. Lu, W. Qin, and G. Cai, "Nonfragile robust model predictive control for uncertain constrained time-delayed system with compensations," *J. Franklin Inst.*, vol. 354, no. 7, pp. 2832–2855, May 2017.

[15] K. Tanaka, T. Ikeda, and H. O. Wang, "Fuzzy regulators and fuzzy observers: Relaxed stability conditions and LMI-based designs," *IEEE Trans. Fuzzy Syst.*, vol. 6, no. 2, pp. 250–265, May 1998.

[16] Q. Lu, P. Shi, H.-K. Lam, and Y. Zhao, "Interval type-2 fuzzy model predictive control of nonlinear networked control systems," *IEEE Trans. Fuzzy Syst.*, vol. 23, no. 6, pp. 2317–2328, Dec. 2015.

[17] Z. Zhong, R.-J. Wai, Z. Shao, and M. Xu, "Reachable set estimation and decentralized controller design for large-scale nonlinear systems with time-varying delay and input constraint," *IEEE Trans. Fuzzy Syst.*, vol. 25, no. 6, pp. 1629–1643, Dec. 2017.

[18] Y. Wang, B. Ren, and Q.-C. Zhong, "Bounded integral controller for nonlinear MIMO systems with inputs constraint," in *Proc. Amer. Control Conf.*, Milwaukee, WI, USA, Jun. 2018, pp. 4688–4693.

[19] Z.-P. Jiang, A. R. Teel, and L. Praly, "Small-gain theorem for ISS systems and applications," *Math. Control, Signals, Syst.*, vol. 7, no. 2, pp. 95–120, Jun. 1994.

[20] Q.-C. Zhong, Y. Wang, and B. Ren, "UDE-based robust droop control of inverters in parallel operation," *IEEE Trans. Ind. Electron.*, vol. 64, no. 9, pp. 7552–7562, Sep. 2017.

[21] Y. Wang, B. Ren, and Q.-C. Zhong, "Bounded UDE-based controller for input constrained systems with uncertainties and disturbances," *IEEE Trans. Ind. Electron.*, early access, Jan. 29, 2020, doi: 10.1109/TIE.2020.2969069.

[22] B. Ren, Y. Wang, and Q.-C. Zhong, "UDE-based control of variable-speed wind turbine systems," *Int. J. Control*, vol. 90, no. 1, pp. 121–136, Jan. 2017.